ОБЪЕДИНЕННЫЙ
ИНСТИТУТ
ЯДЕРНЫХ
ИССЛЕДОВАНИЙ

Дубна

E13-2000-213

I.Chirikov-Zorin, I.Fedorko[1], A.Menzione[2], M.Pikna[1],
I.Sýkora[1], S.Tokár[1]

# METHOD FOR PRECISE ANALYSIS OF THE METAL PACKAGE PHOTOMULTIPLIER SINGLE PHOTOELECTRON SPECTRA

Submitted to «Nuclear Instruments and Methods»

[1]Department of Nuclear Physics, Comenius University,
Mlynska Dolina F1, 84215 Bratislava, Slovakia
[2]Istituto Nazionale di Fisika Nucleare (INFN), Via Livornese,
582A San Piero a Grado, 56010 Pisa, Italy

2000

## 1. Introduction

Photomultipliers (PMTs) are widely used as light detection components of different types of scintillation and Cherenkov detectors (counters, calorimeters, etc.). Some intrinsic spread in characteristic parameters of PMTs, stemming from their multiplicative nature, and their time dependence are among the most serious drawbacks of this type of light detection. Therefore calibration and monitoring of PMT-based spectrometric channels are an inevitable and important part of the experimental setups. Especially important is the absolute calibration, i.e. the measurement of the energy deposited in scintillators in terms of photoelectrons created from the PMT photocathode and captured by the PMT first dynode. The reason is that the basic properties of the scintillating detectors (efficiency, energy resolution, etc.) depend on the number of photoelectrons registered by a detector per unit of deposited energy. In addition the study of the PMT intrinsic parameters is inevitable for a correct estimate of the basic characteristics of such PMT based detectors like calorimeters are (the energy to signal conversion factor, etc). An effective mean of these studies is method of the single photoelectron analysis ([1], [2], [3]). In our previous work [1] we presented a method of PMT calibration and monitoring based on deconvolution of pulse height spectra from a low amplitude pulsed light source which lead to the spectra with a few photoelectrons created on PMT photocathode. A key point of such a method is the choice of the PMT response function. In the work mentioned above we had employed a response function suggested for high resolution PMTs with traditional structure [4] (phototubes with the linear focusing dynodes, box dynodes, venetian-blind dynodes) and satisfactory results had been achieved.

In this work we present the deconvolution method based on the same principles as before [1] for the new types of ultra compact PMTs with the metal channel dynode system [5]. The compactness of these phototubes makes them attractive for applications in high energy physics experiments where experimental setup compactness is of prime importance. The metal channel PMTs are being extensively investigated in high energy physics experiments as the CDF collaboration for the muon detector R&D [6], where the effect of the photoelectron production on PMT first dynode was reported, and ATLAS collaboration for needs of the hadron calorimeter R&D program [7, 8].

## 2. Photomultiplier Response

The basic idea of the calibration and monitoring method consists of a deconvolution of the PMT pulse height spectrum and subsequent use of some of the extracted parameters for calibration purposes. The response function must take care of all important PMT processes. In our approach the PMT is treated as consisting of three independent functional parts:

- The photodetector represented by the photocathode, where the input photon flux is converted into electrons,
- The photoelectron optical input system which accelerates and focuses the photoelectron flux onto the first dynode,
- The electron multiplier consisting of a series of secondary emission electrodes (dynodes), which amplifies the initial charge emitted by the photocathode.

The PMT response function must take into account peculiarities of the PMT structure, and in our case, we will concentrate on the class of metal package PMTs [5]. The global view of such a PMT is shown in Fig. 1, where the structure of a Hamamatsu R5600 PMT is depicted.

The PMT structure can be simplified to two independent stages. The first stage includes the photoconversion and electron collection and the second one includes the charge amplification through the dynode system.

### *2.1. Photoconversion and Electron Multiplication*

A pulsed flux of photons incident on PMT photocathode produces photoelectrons via the photoelectric effect. In many cases the number of photons on the photocathode is a Poisson distributed variable. In addition to this, the conversion of photons into electrons and their subsequent collection by the dynode system is a random binary process. As a result of folding of these two processes the photoelectron distribution again obeys Poisson law:

$$P(n,\mu_{pc}) = \frac{\mu_{pc}^{n} \cdot e^{-\mu_{pc}}}{n!}, \quad \mu_{pc} = n_{ph} \cdot q \tag{1}$$

where $P(n, \mu_{pc})$ is the probability that $n$ photoelectrons will be collected provided that their mean is $\mu_{pc}$, $n_{ph}$ is the mean number of photons hitting photocathode, and $q$ is the quantum efficiency folded with the collection efficiency.

A single photoelectron from the PMT photocathode having been focused and accelerated by the electric field initiate a charge multiplication process in the dynode system as is shown in Fig. 2 for a R5600 PMT. The process finally results in the PMT output charge. The electron avalanche, triggered by one or more photoelectrons, might be described under the following assumptions:

- The emission of secondary electrons is governed by a Poisson law;
- The number of secondaries ($n_S$) depends on the energy ($E$) of the incident electron as $n_S$=const×$E^{\alpha}$, where $\alpha$ is less than 1 (usually $\alpha \approx 0.4$-$0.8$) [4]);
- The energy of secondary electrons is low compared to the energy acquired by the primary from the electric field.

All these peculiarities must be considered for the construction of the response function. As is shown by the simulation [9] the PMT response can be easily found in the case that the number of

secondary electrons on the first dynode is high (>3). In this case, and in the absence of background processes, the charge distribution for the amplification process initiated by one photoelectron can be approximated by a Gaussian distribution. The distribution for the $n$ photoelectron case is a convolution of $n$ one-photoelectron distributions. This idealized case is obtained by summing those distributions with different starting numbers of photoelectrons, weighted by their occurrence probability [1]:

$$S_{ideal}(x) = \sum_{n=0}^{\infty} \frac{\mu_{pc}^{n} e^{-\mu_{pc}}}{n!} \frac{1}{\sigma_1 \sqrt{2\pi n}} \exp\left( -\frac{(x - nQ_1)^2}{2n\sigma_1^2} \right) \tag{2}$$

where $Q_1$ is the average charge at PMT output in the case when one photoelectron was captured by the first dynode and $\sigma_1$ is the standard deviation of the one-photoelectron distribution (in $n$=0 case the limit ($n \to 0$) delta function $\delta(x)$ should be taken instead of Gaussian).

### *2.2. Realistic PMT Response Function*

The basic drawbacks of the function (2) are the following:

- Background processes are not taken into account;
- The one-photoelectron function is assumed to be Gaussian (not true for low values of the secondary emission coefficient on the first dynode);
- No additional processes connected with semi-transparency of the photocathode (like photoelectric effect on the first dynode, focusing and acceleration electrodes) are assumed.

All these issues must be addressed to obtain a realistic response function.

#### *2.2.1. Response Function for the Metal Package PMT*

To create a realistic PMT response function we have made a few natural assumptions.

(i) Only the low charge background processes connected to the leakage current, etc. [1] are assumed for this type of PMT. The processes will lead to the finite width of pedestal and may be represented by the formula:

$$S_{ped}(x) = \frac{1}{\sqrt{2\pi\sigma_0}} \exp\left( -\frac{(x - Q_0)^2}{2\sigma_0^2} \right) \tag{3}$$

with $Q_0$ — the pedestal position and $\sigma_0$ — it's standard deviation.

(ii) The incident light can create photoelectrons from the PMT photocathode, as well as from the first dynode with the occurrence probability for $n$ photoelectrons created from the photocathode and $k$ photoelectrons created from the first dynode given by (1) and the mean number of photoelectrons: $\mu_{pc}$ — from the photocathode and $\mu_1$ — from the first dynode.

(iii) If one or two photoelectrons are collected by the first dynode, then the PMT response is expressed as a sum of responses of secondary electrons created on the first dynode, and for zero and greater than two photoelectrons collected, it is a Gaussian:

$$S_n^{(1)}(x) = \begin{cases} \sum_{m=0}^{\infty} \frac{(nK_1)^m e^{-nK_1}}{m!} S_m^{(2)}(x) & n = 1,2 \\ G(x, Q_0 + nQ_1, \sigma_0^2 + n\sigma_1^2) & n = 0, n \geq 3 \end{cases} \quad (4)$$

where,

- $Q_0$, $\sigma_0$ are the pedestal and its width;
- $Q_1$, $\sigma_1$ are the multiplication process parameters gain, one photoelectron response standard deviation;
- $K_1$ is the secondary emission coefficient of the first dynode;
- $S_m^{(2)}(x)$ is the PMT response for the multiplication process started by an electron from the first dynode;
- $G(x, Q, \sigma^2)$ is a Gaussian distribution with the mean value of $Q$ and dispersion $\sigma^2$;

*Remark.* One photoelectron response is not symmetric and $\sigma_1$ can be different from the standard deviation of the real one photoelectron response. By $\sigma_1$ we mean the quantity:

$$\sigma_1 = \frac{\sigma_n^{real}}{\sqrt{n}} \quad (5)$$

where $\sigma_n^{real}$ is the standard deviation in the case that the number of captured photoelectrons is high enough to give symmetric Gaussian response, practically $n$ (≥3) is sufficient.

For the response of the photoelectrons created on the first dynode the expression analogous to (4) can be written:

$$S_k^{(2)}(x) = \begin{cases} \delta(x) & k = 0 \\ \sum_{m=0}^{\infty} \frac{K_2^m e^{-K_2}}{m!} G(x, Q_0 + mQ_3, \sigma_0^2 + \sigma_3^2) & k = 1 \\ G(x, Q_0 + kQ_2, \sigma_0^2 + \sigma_2^2) & k \geq 2 \end{cases} \quad (6)$$

where $k$ is the number of the photoelectrons created on the first dynode, $K_2$ is the secondary emission coefficient of the second dynode, $Q_2 = Q_1 / K_1$ is the mean charge at the anode initiated by one electron from the first dynode and $\sigma_2$ is corresponding standard deviation, $Q_3 = Q_2 / K_2$ is the mean charge at the anode initiated by one electron from the second dynode and $\sigma_3$ is its standard deviation.

All other processes can be neglected for the moment. The output charge spectrum for the case in which $n$ photoelectrons have been created on the photocathode and $k$ on the first dynode, can be expressed as the following convolution:

$$S_{real}(x) = \sum_{n,k=0}^{\infty} \frac{\mu_{pc}^n e^{-\mu_{pc}}}{n!} \frac{\mu_1^k e^{-\mu_1}}{k!} \cdot \int dx' S_n^{(1)}(x') S_k^{(2)}(x - x') \quad (7)$$

where

- $\mu_{pc}$ — the light source intensity expressed in number of photoelectrons captured by the PMT dynode system;

- $\mu_1$ — the number of photoelectrons created on the first dynode and captured by the following dynode system.

The formula shown above presumes that in the case of two or less photoelectrons collected by the first dynode the PMT response is not a Gaussian. In this case the response is expressed as a sum of the responses corresponding to different numbers of electrons collected by the second dynode and weighted by the corresponding Poisson factors — the number of secondaries created on the dynode by one electron is governed by Poisson statistics. From the simulation of the R5600 response (see bellow) we can conclude, that at least at high gain (in our case at the PMT voltage ≥800 *V*), it is sufficient to expand the PMT response in case when 1 or 2 photoelectrons are captured. The convolution

$$\tilde{S}_{nk}(x) = \int dx' S_n^{(1)}(x') S_k^{(2)}(x - x') \tag{8}$$

can be expressed as follows:

$$\tilde{S}_{nk}(x) = \begin{cases} \sum_{m=0}^{\infty} \frac{(nK_1)^m e^{-nK_1}}{m!} G(x, Q_0 + (m+k)Q_2, \sigma_0^2 + (m+k)\sigma_2^2) & n = 1,2 \\ G(x, Q_0 + nQ_1 + kQ_2, \sigma_0^2 + n\sigma_1^2 + k\sigma_2^2) & n = 0, n \geq 3 \end{cases} \tag{9}$$

The response function $S_{\text{real}}(x)$ can be further generalized if the effect of "fly through" photoelectrons are taken into account. Those are the photoelectrons from the photocathode collected on the second dynode instead in the first one.

### *2.2.2. Limit Spectrum*

For many applications it is important to consider the limit of the real spectrum (7) for high intensity light sources ($\mu_{pc} \to \infty$). At large values of $\mu_{pc}$ the corresponding Poisson distribution present in (7) becomes Gaussian:

$$\frac{\mu_{pc}^n \exp(-\mu_{pc})}{n!} \underset{\mu_{pc} \to \infty}{\to} \frac{\exp\left(-\frac{(n-\mu_{pc})^2}{2\mu_{pc}}\right)}{\sqrt{2\pi\mu_{pc}}} \tag{10}$$

The same is true for the Poisson factor with $\mu_1$. Using the Gaussian approximation for the Poisson factors in (7) the PMT response from $n$ photoelectrons from the photocathode and $k$ photoelectrons from the first dynode can be represented by a Gaussian:

$$\tilde{S}_{nk}(x) \underset{\mu_{pc} \to \infty}{\to} G(x, Q_0 + nQ_1 + kQ_2, \mu_{pc}\sigma_1^2 + \mu_1\sigma_2^2) \tag{11}$$

As in the summation present in (7) only $n$ from $\left(\mu_{pc}-\sqrt{\mu_{pc}},\mu_{pc}+\sqrt{\mu_{pc}}\right)$ and $k$ from $\left(\mu_1-\sqrt{\mu_1},\mu_1+\sqrt{\mu_1}\right)$ will effectively contribute. Replacing in (7) the summation over $n$ and $k$ by integration, the PMT response function goes to the limit spectrum:

$$S_{real}(x) \underset{\mu_{pc}\to\infty}{\to} S_\infty(x)=\frac{1}{\sqrt{2\pi}\sigma_\infty}\exp\left(\frac{(x-Q_0-Q_\infty)^2}{2\sigma_\infty^2}\right) \tag{12}$$

where

$$Q_\infty=\mu_{pc}Q_1+\mu_1Q_2=\mu_{pc}Q_1\left(1+\frac{\varepsilon}{K_1}\right) \tag{13}$$

$$\sigma_\infty=\sqrt{\sigma_0^2+\mu_{pc}(\sigma_1^2+Q_1^2)+\mu_1(\sigma_2^2+Q_2^2)} \underset{\varepsilon<0.1}{\to} \sqrt{\mu_{pc}(\sigma_1^2+Q_1^2)} \tag{14}$$

where $\varepsilon=\mu_1/\mu_{pc}$ and $K_1$ is secondary emission coefficient on the first dynode.

It is useful to find a relation between the limit spectrum parameters $(Q_\infty,\sigma_\infty)$ and the mean number of photoelectrons $(\mu_{pc},\mu_1)$. From (13) and (14) it follows:

$$\mu_{pc}=f_{pmt}\frac{Q_\infty^2}{\sigma_\infty^2} \tag{15}$$

$$f_{pmt}=\frac{\sigma_1^2+\varepsilon\sigma_2^2+Q_1^2\left(1+\dfrac{\varepsilon}{K_1^2}\right)}{Q_1^2\left(1+\dfrac{\varepsilon}{K_1^2}\right)^2} \to 1+\frac{\sigma_1^2}{Q_1^2} \tag{16}$$

The last relation is justified if the effect on the first dynode is small ($\varepsilon < 0.1$). The factor $f_{pmt}$, called usually the excess factor, depends on the single photoelectron parameters (one photoelectron resolution) of the PMT in question, and reflects a quality of PMT. The second term in (16) is a contribution of the fluctuations caused by dynode system. It is desirable to have this contribution to PMT output charge fluctuations as low as possible. In ideal case the charge fluctuations are fully determined by photocathode fluctuations and in this case $f_{pmt}$ =1. However, the typical values of $f_{pmt}$ are expected to vary between 1.15 to 1.50.

### *2.2.3. Relation Between Amplification Process Parameters*

A realistic PMT response function like the one given by (7) is always expressed through several parameters: $Q_0,\sigma_0,Q_1,\sigma_1,Q_2,\sigma_2,\mu_{pc}$ and $\mu_1$. Some of the parameters are clearly independent, as $Q_0$ and $\sigma_0$ (defining pedestal position and width, $\mu_{pc}$ and $\mu_1$ — characterizing the light source intensity in combination with photon to electron conversion at the photocathode and first dynode. The other parameters $Q_1$, $\sigma_1$, $Q_2$, $\sigma_2$, characterizing the charge multiplication process in the dynode system, are not fully independent. It is important to know what are their mutual relationships.

Starting with the assumption that the PMT has an $N$ stage dynode system and that one electron hitting the $i^{th}$ dynode will create an average $k_i$ of secondary electrons. If we denote as $Q_j$ the mean anode charge initiated by one electron captured by the $j^{th}$ dynode (the charge multiplication starts from the $j^{th}$ dynode), then it is easy to express $Q_j$ via the coefficients $k_i$ and elementary charge $e$:

$$Q_j = e \cdot k_j \cdot k_{j+1} \cdots k_N = e \cdot \prod_{i=j}^{N} k_i \tag{17}$$

The variance $\sigma_j^2$ of the anode charge initiated by one electron can be expressed as [10]:

$$\sigma_j^2 = Q_j^2 \left( \left( \frac{\delta_j}{k_j} \right)^2 + \frac{1}{k_j} \left( \frac{\delta_{j+1}}{k_{j+1}} \right)^2 + \ldots + \frac{1}{k_j k_{j+1} \cdots k_N} \left( \frac{\delta_N}{k_N} \right)^2 \right) \tag{18}$$

where $\delta_i (i = 1,\ldots,N)$ is the standard deviation of the number of secondary electrons created from the $i^{th}$ dynode by one electron.

The validity of the relation (18) is shown for the case $N$=2 in Appendix 1 and can be easily generalized for the general case of $N$ dynodes. Simplification of the formulae (18) can be achieved if we assume that the standard deviations $\delta_i$ are governed by a Poisson law:

$$\delta_i = \sqrt{k_i} \tag{19}$$

Assuming (19) the relation between $\sigma_j$ and $Q_j$ reads

$$\sigma_j^2 = Q_j^2 \left( \frac{1}{k_j} + \frac{1}{k_j k_{j+1}} + \ldots + \frac{1}{k_j \cdots k_N} \right) \tag{20}$$

At a fixed voltage the factor in brackets is a PMT constant which can be determined for any voltage divider ratio. The simplest expression of (20) is in case of the divider 1: 1: …: 1, where for all dynodes $k_i$=$k$.

The dynode secondary emission coefficients are essentially determined by inter-dynode voltages [11] and for the $i^{th}$ dynode coefficient one can write

$$k_i = \gamma U_i^{\alpha} = \gamma \left( \frac{r_i}{\sum_{j=1}^{N+1} r_j} \right)^{\alpha} U^{\alpha} \tag{21}$$

where $U_i$ is the inter-dynode voltage (between dynode $i$ - 1 and $i$, $U$ is the overall voltage between photocathode and anode, $r_i (i = 1,\ldots,N+1)$ is the voltage divider ratios, $N$ is the number of dynodes, $\alpha$ is a material dependent coefficient (constant for a given PMT) and $\gamma$ is also a PMT constant that can be determined from gain measurement. Using (21) the PMT gain reads

$$G = \prod_{i=1}^{N} k_i = \frac{\gamma^N \cdot \prod_{i=1}^{N} r_i^{\alpha}}{\left( \sum_{i=1}^{N+1} r_i \right)^{\alpha N}} \cdot U^{\alpha N} \tag{22}$$

If the voltage divider is fixed, then the gain $G$ is an exponent function of the voltage $U$ and the formula (22) can be used to find the PMT constants $\alpha$ and $\gamma$ and via (21) also the secondary emission coefficients. Having determined the coefficients $k_i$ by an independent way we can fix the parameters $Q_1, \sigma_1, Q_2$ and $\sigma_2$ using (17), (20) and the relation between gain $G$ and parameter $Q_1$: $G$=$Q_1/e$.

On the other hand it should be stressed that the relations like (20) are valid only for an ideal case. In a real case inhomogeneities of various kinds (like the dynode surface inhomogeneity, collection inefficiency, etc.) will make the value of standard deviation broader than in the ideal case. In our analysis we usually use three of the parameters: $Q_1$, $\sigma_1$, $k_1$ =$Q_1/Q_2$ finding the fourth of

them on the basis of (20). On the other hand a possibility to free all four parameters has been conserved as well as a possibility to fix all possible parameters.

## 3. Results of Analysis

To verify the response function we took and analyzed a series of faint light (a few photoelectrons) spectra under different conditions. These spectra were analyzed by means of the response function (7), for the eight dynode R5600 Hamamatsu photomultipliers. The results of the analysis are summarized bellow.

### *3.1. Experimental Setup*

Our analytical method based on the deconvolution of the LED spectra using the response function (7) was tested on the experimental data. The block diagram of the experimental setup is shown in Fig. 3. The fast AlGaAs LED HLMP8100 ("Hewlett Packard") was used as a pulsed light source. The LED was driven by a pulse generator (GEN) with a short pulse width ($\approx$10 *ns*). An optical fiber was used to transmit light from the LED to the PMT. The photon flux incident on the photocathode was tuned by changing the supply voltage to the LED. The analog signal from the PMT was amplified by a preamplifier Model 777 "Phillips Scientific" and measured by an ADC (LeCroy 2249A). The preamplifier amplification coefficient was 18.4 and width of the gate signal was 80 *ns*. The output information from the ADC was read by means of PC computer.

### *3.2. Dependence of the Output Spectrum Parameters on PMT Voltage*

To find the dependence of the basic parameters on the voltage applied to the PMT, we took the spectra with the same pulsed light source intensity but at different high voltages. The results for the R5600 are shown in Tables 1 and 2 and in Figs. 4 and 5. In Table 1 the deconvoluted parameters of the spectra taken at different PMT voltages are shown for the case when the first dynode secondary emission coefficient $K_1$ is calculated from $Q_1$ using the relation (17). Table 2 presents the results of analysis of the same spectra but for the case when $K_1$ is independent of $Q_1$. In Fig. 4 the deconvoluted spectrum taken at 1000 *V* is shown. In Fig. 5a-d the essential part of the deconvoluted spectra taken at 800 *V*, 850 *V*, 900 *V* and 950 *V* are shown in linear scale. We can clearly see from these figures the presence of the first dynode effect (the first peak after pedestal). As will be shown bellow, this effect can be interpreted as caused by the photoelectric effect on the first dynode. It can be seen from Table 1,2 and Fig. 4, 5, the parameter $Q_1$ (essentially gain expressed in the ADC channels) increases with the voltage as expected. The first dynode secondary emission coefficient $K_1$ also shows the same behavior. A small increase in the mean number of photoelectrons ($\mu_{pc}$) with voltage is seen. This effect can be explained by the fact that even at voltages higher than the plateau threshold, the voltage at which collection efficiency reaches its plateau, there is an increase of the photoelectron collection efficiency. This effect is also observed at photocathode current measurement in the mode with the continuous light source [8] as a slight increase of photocathode sensitivity with voltage between photocathode and first dynode. This is an edge effect, which can be especially visible for the PMTs with a small effective photocathode, as the effect should be proportional to the ratio of the photocathode circumference and surface, i.e. it should be proportional to $1/R$, where $R$ is the photocathode radius. From Tables 1,2 we also see that the ratio $\mu_1/\mu_{pc}$ is essentially stable. The fluctuations of this ratio could arise from the definition of the first dynode peak area. This systematic error found from the $\mu_1/\mu_{pc}$ fluctuation is about 5-7%. From the dependence of parameter $Q_1$ on high voltage, the secondary emission exponent $\alpha$ can be found. We

fit $Q_1$ data from Table 2 with formula (22) and obtained $\alpha$=0.874±0.007. The result of this fit is shown in Fig. 6. The coefficient is important in the case when a non-uniform voltage divider is used.

### *3.3. Output Spectrum Parameters vs. First Dynode Voltage*

To understand the nature of the first dynode effect we have taken a series of spectra with different voltages between first dynode and photocathode ($U_1$). The voltage $U_1$ is a sensitive parameter that enables us to distinguish between the photoelectric effect on the first dynode and direct capture of photoelectrons by the second dynode. In case of the latter effect a photoelectron created from the photocathode is missing the first dynode and is captured directly by the second dynode. If the first dynode effect is caused by the photoelectrons directly captured by second dynode, then the position of the first dynode peak ($Q_2$) will move with the voltage $U_1$ as $Q_2 \sim (U_1+U_2)^{\alpha}$, while if it is caused by the photoelectric effect on first dynode, then this peak will not move, as in this case $Q_2 = \sim U_2^{\alpha}$ and $U_2$ does not change. To exclude possible systematic uncertainties (determining the first dynode peak area, etc.) we fixed the secondary emission coefficient on the first dynode $K_1$ via formula (21) with $\gamma \approx 36.1$, $\alpha \approx 0.87$ and voltage expressed in *kV*. The results of analysis are presented in Fig. 7 and Table 3 from where it can be seen that the position of the first dynode peak ($Q_2$) does not move with the voltage $U_1$. In case of the second dynode direct capture effect, more than 50% increase of ($Q_2$ is expected when $U_1$ is increased form 139 *V* to 228 *V*. Therefore we conclude that the first dynode peak is caused mainly by the photoelectric effect on first dynode. From the results we also see that $\chi^2$ of the fit increases with increasing voltage $U_1$ (increasing divider non-uniformity). Fig. 7 neatly shows that the discrepancy is in the region of small amplitudes (left side of the one photoelectron distribution), where an excess is of real events over the expected ones is observed. The discrepancy at high values of voltage between the photocathode and first dynode can be caused by some presence of direct capture of photoelectrons by second dynode and the above mentioned edge effect. In the former case, the photoelectrons from photocathode are captured by second dynode and are accelerated by bigger voltage than the photoelectrons from first dynode. It will lead to an enhanced signal if compared with that initiated by the photoelectrons from the first dynode. In the latter case, the photoelectrons from photocathode may produce less secondary electrons on first dynode and that would lead to an enhanced left tail of the one-photoelectron distribution.

### *3.4. Comparison of the experimental spectra with the simulation*

For better understanding of the observed spectra and results of their analysis we compared them with the spectra obtain with the simulation. Details of the code were published elsewhere [9]. Here we only give the main features of the code:

- Photoconversion is governed by Poisson law and can occur on photocathode and on first dynode.
- Charge multiplication in PMT dynode system is also governed by Poisson law.
- Possible inhomogeneity of dynode system, i.e. dependence of dynode secondary emission coefficient on place of incidence, has been introduced into the code.
- Direct capture of photocathode electrons by second dynode has been included.

First of all we simulated an 8-staged PMT assuming that the charge multiplication process is an ideal one, i.e. production of secondaries obeys Poisson law, no inhomogeneities are present, photoelectrons are created only on photocathode and collection efficiency of dynode system is 100%. We carried out the simulation for two PMT gains corresponding to two voltages of the

tested R5600 PMT — 850 *V* and 1000 *V*. The main purpose of these simulations was to investigate how the form of PMT response depends on number of photoelectrons initiating it. The results are presented in Fig. 8, where the charge distributions initiated by $n = 0, 1, 2, 3, 4$ and 6 photoelectrons are shown for the gain at 850 *V*. A similar results have been obtained also at 1000 *V*. We can conclude that for gains greater than $10^6$ the "idealized" PMT response is symmetric (Gaussian) if charge distribution is initiated by 3 or more photoelectrons. One can expect that inhomogeneities (in a real case) will not change this fact dramatically, i.e. our choice to expand the PMT response, in cases when it is initiated by 1 or 2 photoelectrons, is justified.

In a second phase we have tried to reproduce a real response of the tested PMT. In Fig. 9 the experimental spectra taken by the R5600 PMT taken at 850 *V* and 1000 *V* have been compared with those obtained in the simulation. The spectra were simulated under two different sets of conditions. In the first case an idealized response of PMT was assumed – neither direct capture of photoelectrons by second dynode nor dynode inhomogeneity has been included. In the second case more realistic conditions were treated – both above mentioned effects have been included. The spectra obtained for "idealized" dotted line conditions do not reproduce the experimental data properly. On the other hand the spectra obtained under a more realistic conditions (dashed line) are in an excellent agreement with the observed ones (thick line). This good agreement was achieved for 17% dynode inhomogeneity and approximately 30% direct capture effect if compared with the photoelectric effect on first dynode. It should be stressed that the second dynode direct capture effect can "arise" as a result of systematics connected with behavior of left tail of one photoelectron response or right tail of the first dynode photoelectron response. In any case it appears that the dominant role in the first dynode effect plays the photoconversion on the first dynode.

It should be noted that at the simulation input we used as input parameters only: the PMT gain, voltage divider ratios (1: 1: ...:1), ADC resolution (10 bits, 0.25 *pC/channel*) and position of pedestal.

## 4. Conclusions

We present the results showing that the deconvolution method, for analysis of single photoelectron spectra of metal package photomultipliers, works well, at least for the class of the above mentioned PMTs.

The PMT response function employed in this method describes in an adequate way processes in the metal package photomultiplier and enables to watch also subtle effects as the photoconversion on first dynode and/or direct capture of photoelectrons by second dynode.

The method uses only the elementary physical principles and therefore can be easily adapted to other types of photomultipliers.

Our method enables to find important PMT parameters like the position of the charge distribution initiated by one photoelectron (PMT gain), its standard deviation, etc. (c.f. part 2.3). On the basis of these parameters we can calculate the PMT access factors needed in finding the relation between the mean numbers of photoelectrons and parameters of an experimental spectrum with high input light signal (15, 16), and it enables us to calculate the energy-to-signal conversion factor (number of photoelectrons per *GeV*) for PMT based calorimeters.

The method can be used as a calibration and monitoring tool for studying stability in time of a photomultiplier using the gain (parameter $Q_1$).

## 5. Acknowledgements

The authors want to thank S. Leone (INFN Pisa) for an accurate reading of the manuscript and for valuable remarks and P. Strmen (Comenius Univ., Bratislava) for technical help.

## Appendix. Fluctuations in a Two Dynode System

In the case of a two-dynode system the anode charge can be expressed as

$$q = \sum_{i=1}^{q_1} q_2^{(i)} \tag{23}$$

where $q_1$ is the number of electrons created from the first dynode and $q_2^{(i)}$ is the number of electrons created from the second dynode by $i^{th}$ electron from the first dynode. The mean value of charge $q$ is easy to find:

$$\bar{q} = E\left(\sum_{i=1}^{q_1} q_2^{(i)}\right) = \sum_{m=0}^{\infty} P_m^{(1)} \sum_{i=1}^{m} E\left(q_2^{(i)}\right) = \sum_{m=0}^{\infty} P_m^{(1)} m k_2 = k_1 k_2 \tag{24}$$

where $E$ is the expected value, $P_m^{(1)}$ is the probability to have $m$ electrons created from the 1st dynode. We used the fact that each of the 1st dynode electrons creates from the 2nd dynode the same average number of electrons $k^2$.

The dispersion $\sigma_q^2$ can be expressed as

$$\sigma_q^2 = E\left(q^2\right) - k_1^2 k_2^2 \tag{25}$$

where

$$E\left(q^2\right) = E\left(\sum_{i,j=1}^{q_1} q_2^{(i)} q_2^{(j)}\right) = \sum_{m=02}^{\infty} P_m^{(1)} \sum_{i,j=1}^{m} E\left(q_2^{(i)} q_2^{(j)}\right) = \sum_{m=0}^{\infty} P_m^{(1)} \left(m\overline{q_2^2} + m(m-1)k_2^2\right) =$$

$$= k_1 \overline{q_2^2} + k_2^2 \overline{q_1^2} - k_1 k_2^2 = k_1 \sigma_2^2 + k_2 \overline{q_1^2} \tag{26}$$

Combining (25) and (26) we have

$$\sigma_q^2 = (k_1 k_2)^2 \left[\left(\frac{\sigma_1}{k_1}\right)^2 + \frac{1}{k_1}\left(\frac{\sigma_2}{k_2}\right)^2\right] \tag{27}$$

Generalization of (27) to the general case of $N$ dynodes is straightforward and leads to the relation (18).

*Table 1*: Dependence of the R5600 PMT output spectrum parameters on the voltage applied to the PMT. The fitting function (7) has been applied with the ratio $\sigma_3/Q_3 = \sigma_2/Q_2$ and $K_1$ calculated from $Q_1$.

| $U$ | 800 $V$ | 850 $V$ | 900 $V$ | 950 $V$ | 1 $kV$ |
|---|---|---|---|---|---|
| $Q_0$ | 13.53±0.022 | 13.59±0.017 | 13.59±0.015 | 13.45±0.018 | 13.54±0.015 |
| $\sigma_0$ | 0.47±0.017 | 0.47±0.015 | 0.49±0.015 | 0.67±0.02 | 0.53±0.017 |
| $Q_1$ | 15.20±0.04 | 23.32±0.09 | 35.24±0.26 | 50.52±0.37 | 72.76±0.63 |
| $\sigma_1$ | 7.80±0.16 | 11.32±0.23 | 16.92±0.31 | 24.73±0.47 | 32.04±0.60 |
| $K_1$ | 5.74 | 5.97 | 6.23 | 6.58 | 7.06 |
| $\sigma_2$ | 1.60±0.06 | 2.40±0.09 | 3.07±0.08 | 5.55±0.26 | 6.10±0.13 |
| $\mu_{pc}$ | 1.446±0.009 | 1.459±0.010 | 1.466±0.015 | 1.520±0.014 | 1.519±0.017 |
| $\mu_1$ | 0.832±0.035 | 0.867±0.03 | 0.892±0.025 | 0.883±0.024 | 0.949±0.023 |
| $\chi^2$ | 77.9/126 | 134.8/181 | 260.0/287 | 413.7/388 | 533.0/493 |
| $\mu_1/\mu_{pc}$ | 57.5% | 59.4% | 60.8% | 58.1% | 62.5% |

*Table 2*: Dependence of the R5600 PMT output spectrum parameters on the voltage $U$ applied to the PMT. The fitting function (7) has been applied with the ratio $\sigma_3/Q_3=\sigma_2/Q_2$ and $K_1$ independent of $Q_1$.

| $U$ | 800 $V$ | 850 $V$ | 900 $V$ | 950 $V$ | 1 $kV$ |
|---|---|---|---|---|---|
| $Q_0$ | 13.55±0.021 | 13.59±0.017 | 13.59±0.015 | 13.45±0.018 | 13.54±0.015 |
| $\sigma_0$ | 0.47±0.017 | 0.47±0.014 | 0.49±0.015 | 0.67±0.02 | 0.53±0.017 |
| $Q_1$ | 15.13±0.17 | 23.18±0.22 | 35.17±0.26 | 50.48±0.38 | 72.63±0.61 |
| $\sigma_1$ | 7.87±0.16 | 11.46±0.24 | 17.00±0.30 | 24.75±0.48 | 32.19±0.61 |
| $K_1$ | 5.53±0.14 | 5.80±0.11 | 6.33±0.09 | 6.70±0.09 | 7.06±0.08 |
| $\sigma_2$ | 1.62±0.07 | 2.46±0.10 | 3.10±0.08 | 5.92±0.25 | 6.16±0.13 |
| $\mu_{pc}$ | 1.450±0.023 | 1.464±0.019 | 1.468±0.015 | 1.521±0.015 | 1.520±0.012 |
| $\mu_1$ | 0.804±0.037 | 0.841±0.03 | 0.879±0.025 | 0.880±0.025 | 0.936±0.023 |
| $\chi^2$ | 73.9/125 | 125.1/180 | 258.2/286 | 413.3/387 | 530.6/492 |
| $\mu_1/\mu_{pc}$ | 55.4% | 57.4% | 59.9% | 57.9% | 61.6% |

*Table 3*: Dependence of the R5600 PMT parameters vs. the voltage between photocathode and 1st dynode is $U_1$ (changed from 139 $V$ to 228 $V$). The voltage between the 1st dynode and anode was fixed at 861 $V$. $K_1$ is fixed using formula (21) with the secondary emission exponent $\alpha$=0.87 and voltage divider ratios: $U_1$: ... 115:115:55; the last voltage in this ratio is the voltage between the last dynode and anode.

| $U_1$ | 139 $V$ | 185 $V$ | 205 $V$ | 228 $V$ |
|---|---|---|---|---|
| $Q_0$ | 11.57±0.020 | 11.65±0.019 | 11.66±0.018 | 11.59±0.013 |
| $\sigma_0$ | 0.66±0.013 | 0.65±0.014 | 0.66±0.013 | 0.48±0.014 |
| $Q_1$ | 82.02±0.46 | 102.92±0.55 | 112.15±0.61 | 123.08±0.69 |
| $\sigma_1$ | 39.81±0.72 | 47.53±0.95 | 52.98±1.05 | 56.98±1.17 |
| $K_1$ | 6.49 | 8.31 | 9.08 | 9.97 |
| $\sigma_2$ | 8.25±0.16 | 10.72±0.17 | 12.07±0.17 | 12.08±0.14 |
| $\mu$ | 1.254±0.010 | 1.294±0.010 | 1.276±0.010 | 1.269±0.010 |
| $\mu_1$ | 0.601±0.013 | 0.583±0.013 | 0.555±0.013 | 0.551±0.014 |
| $\chi^2$ | 751.6/549 | 729.7/670 | 907.2/681 | 1464.5/732 |

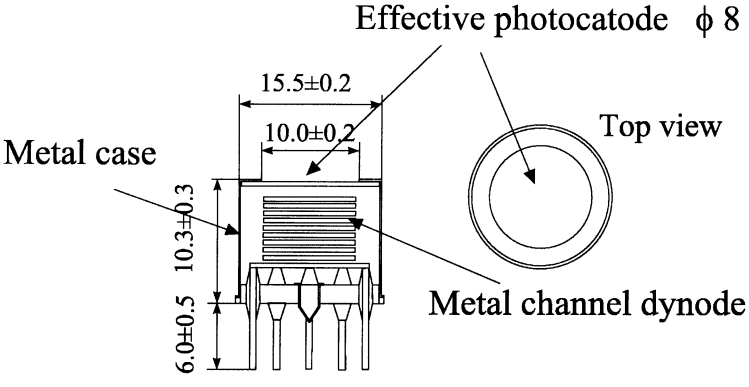


Figure 1: The overall view of a Hamamatsu R5600 photomultilier.

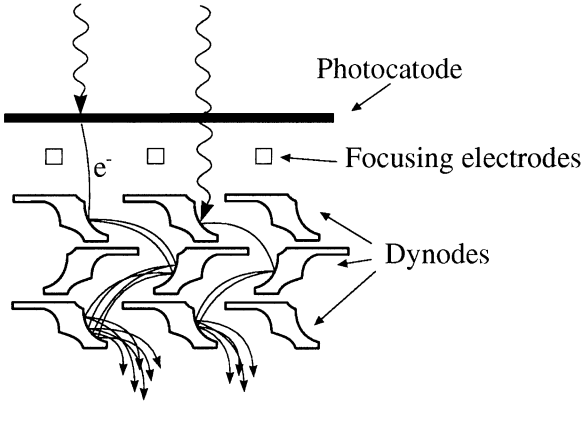


Figure 2: Charge multiplication process in the metal channel dynode photomultiplier.

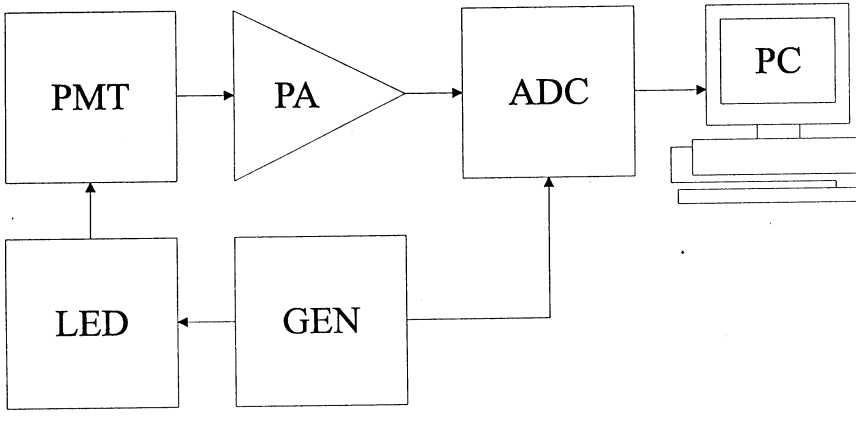


Figure 3: Block scheme of the experimental setup for the measurement of single photoelectron spectra.

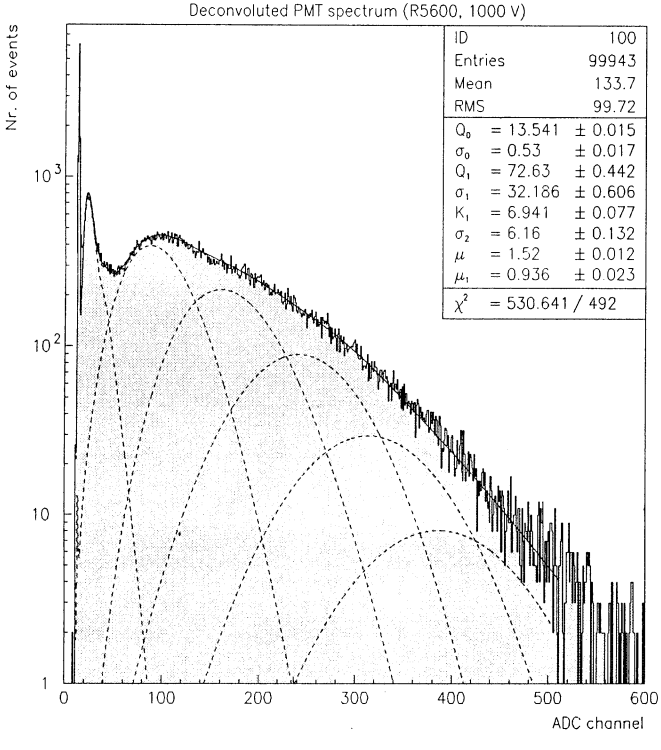


Figure 4: The deconvoluted LED initiated PMT pulse height spectrum taken at 1000 V by a Hamamatsu R5600 photomultilier. The first dynode secondary emission coefficient $K_1$ is treated as an independent parameter.

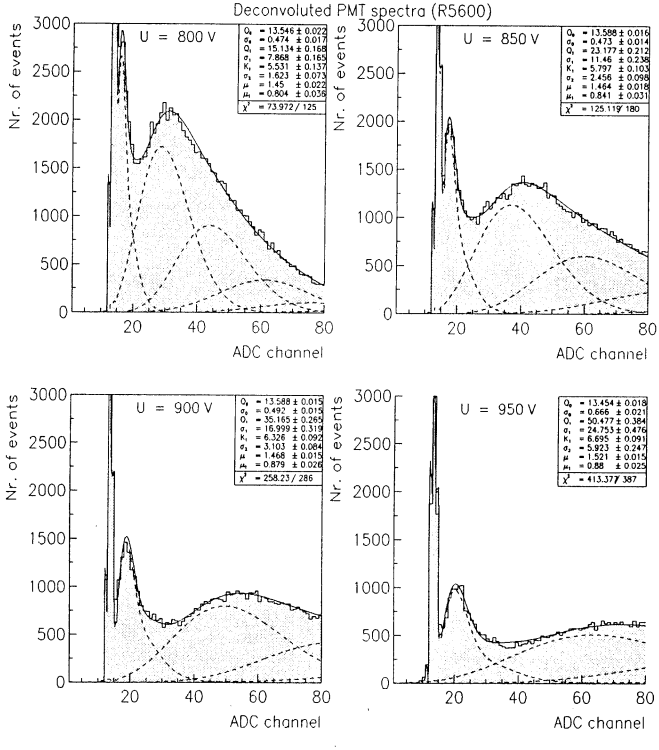


Figure 5: The deconvoluted LED initiated PMT pulse height spectra taken at 800 V, 850 V,900 V, and 950 V by a Hamamatsu R5600 photomultiplier. The same conditions are valid as in the case of the spectrum in Fig. 4.

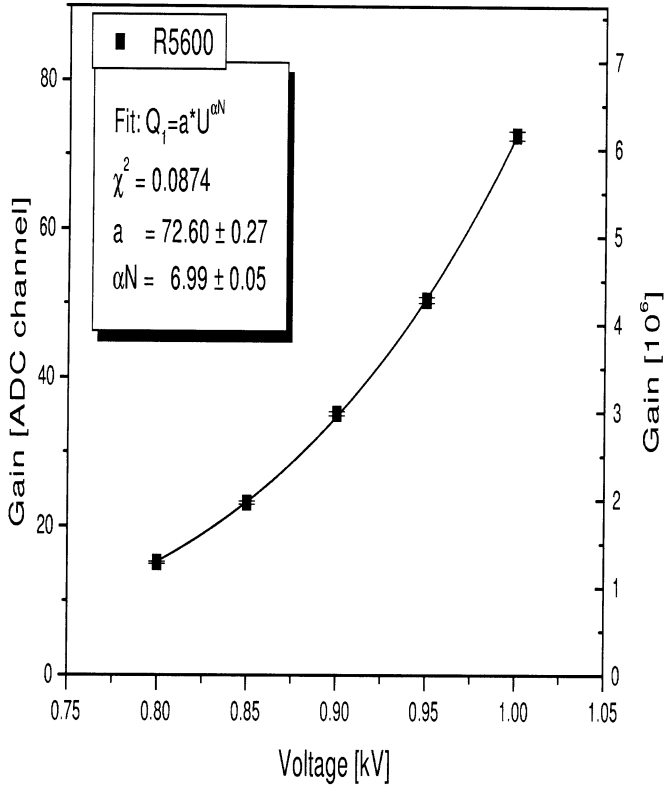


Figure 6: Dependencies of the gain (parameter $Q_1$) on voltage for the R5600 photomultiplier

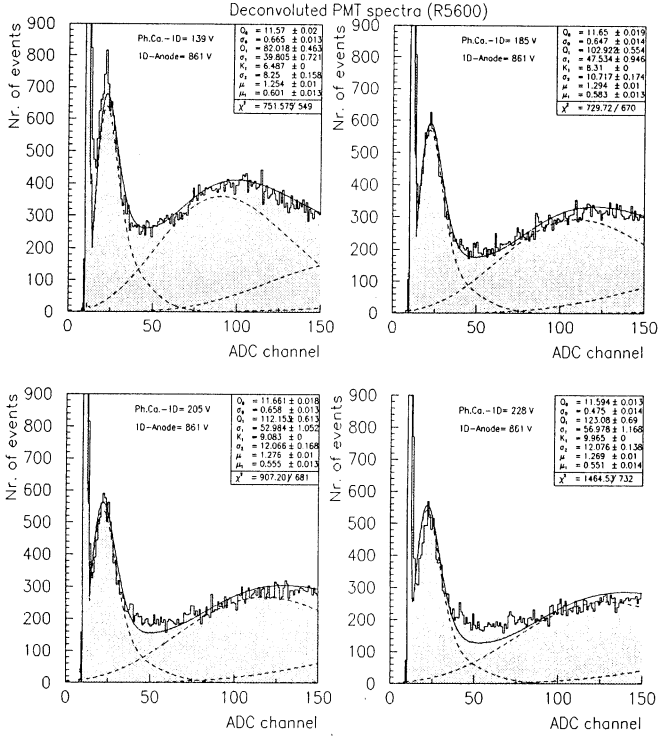


Figure 7: The deconvoluted LED initiated PMT pulse height spectra taken at different first dynode voltages (139 V, 185 V, 205 V, and 228V) by a Hamamatsu R5600. The voltage between the first dynode and anode was fixed at 861 V.

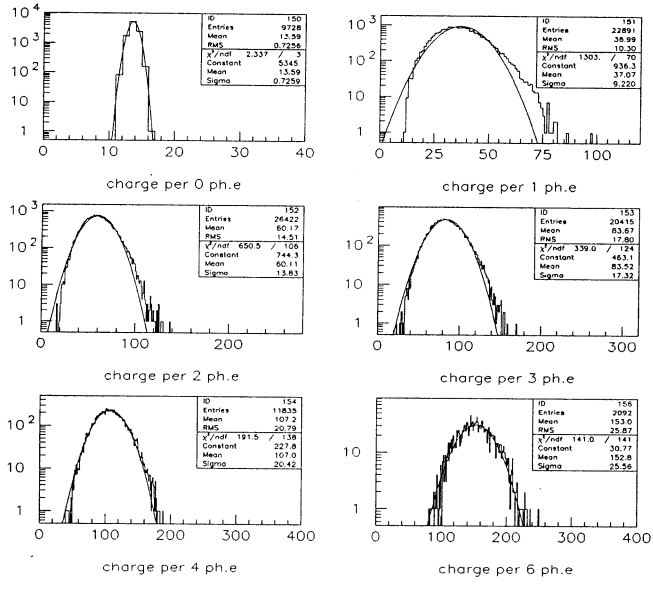


Figure 8: The simulated PMT responses at 850 $V$ initiated by different number of photoelectrons - $n = 0, 1, 2, 3, 4$ and 6.

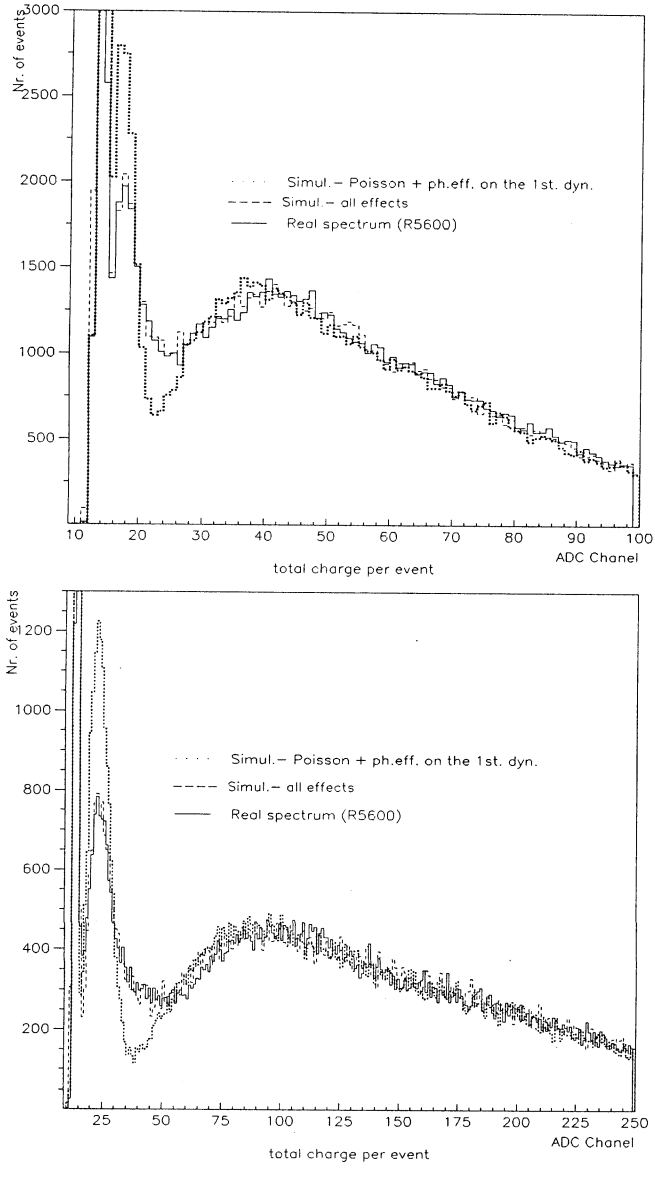


Figure 9: The spectra taken at 850 V and 1000 V taken by the R5600 PMT(black line) are compared with the simulated ones .

## References


[1] E. H. Bellamy, I. Chirikov-Zorin, S. Tokar, et al, Absolute Calibration and Monitoring of a Spectrometric Channel Using a Photomultiplier, Nucl Instrum Meth A339, 468-476(1994)

[2] Response function for Analysis of the Metal Package Photomultiplier Single Photoelectron Spectra. By: S. Tokar, I. Sykora, M. Pikna, I. Chirikov-Zorin, J.A. Budagov, and A. Menzione, Acta Physica Univ. Comenianae,Vol. XL(1999) 105-122

[3] ATL-TILECAL-99-005 (ATL-COM-TILECAL-99-004)[1], Single Photoelectron Spectra Analysis for the Metal Package Photomultiplier, by: S. Tokar, I. Sykora, M. Pikna, I. Chirikov-Zorin, and A. Menzione, 16 Feb 1999, CERN

[4] Photomultiplier Tubes, principles an applications (Handbook), Phillips Photonics, 1994 France

[5] Y. Yoshizawa, J.Takeuchi, The latest vacuum photodetector, Nucl Instrum Meth A387 (1997) p. 33

[6] Ju. A. Budagov et al., Long Scintillation Counters with the Shift-Spectrum Fiber Light Guides, JINR, 13-98-304,DUBNA (1998)

[7] ATLAS Collaboration, ATLAS Technical Proposal for a General-Purpose pp experiment at the Large Hadron Collider, CERN/LHCC/ 94-93, CERN, Geneva, Switzerland. ATLAS Collaboration, ATLAS TILE Calorimeter Technical Design Report, CERN/LHCC/96-42, ATLAS TDR 3, 1996, CERN, Geneva, Switzerland

[8] a) ATL-TILECAL-98-156. (ATL-L-PN-156)[1]. Measurement of 20 Hamamatsu R-5900 Photomultiplier Tubes for ATLAS TileCal Module-0. by: Ames,E; et al. - 23 Mar 1998

b) ATL-TILECAL-98-152. (ATL-L-PN-152)[1]. Light yield of the 1997 Extended Barrels Module 0 from Cs data with nominal PMT settings. by: S.Bravo and M.Delfino; - 23 Mar 1998

c) ATL-TILECAL-98-148. (ATL-L-PN-148)[1]. Technical characteristics of the prototype of the TILECAL photomultipliers test-bench. by: M.Crouau G.Montarou D.Rey; - 23 Mar 1998

d) ATL-TILECAL-97-131. (ATL-L-PN-131)[1]. Study of the light produced in PMT/light guide region of Tile barrel Module 0. by: Henriques,A; Nessi,M; Poulsen,U; - 28 Nov 1997

e) ATL-TILECAL-97-129. (ATL-L-PN-129)[1]. Characterization of 8-stages Hamamatsu R5900 photomultipliers for the TILE calorimeter. by: Crouau,M; Grenier,P; Montarou,G; Poirot,S; Vazeille,F; - 20 Oct 1997

f) ATL-TILECAL-97-120. (ATL-L-PN-120)[1]. Light produced in the Fibre bundle/Light guide/PMT region of the Tile Calorimeter prototype. by: Di Girolamo,B; Henriques,A; Maio,A; Santos,J; Varanda,M; - 25 Jun 1997

g) ATL-TILECAL-97-117. (ATL-L-PN-117)[1]. Study of the charge spectra generated by photomultipliers. by: Cavasinni,V; et al. - 06 Jun 1997

h) ATL-TILECAL-97-108. (ATL-L-PN-108)[1]. Characterization of the Hamamatsu 10-stages R5900 photomultipliers at Clermont for the TILE calorimeter. by: Bouhemaid,N; Crouau,M; Gil Botella,A; Gonzalez de la Hoz; Grenier,P; Montarou,G; Muanza,G.S; Poirot,S; Vazeille,F; - 28 Apr 1997

i) ATL-TILECAL-96-097. (ATL-L-PN-97)[1]. Characterization of the new R5900 Hamamatsu photomultiplier in Pisa. by: Beschastnov, P; Cavasinni, V; Cologna, S; Del Prete, T; Di Girolamo, B; Mazzoni, E; - 09 Dec 1996

j) ATL-TILECAL-96-083. (ATL-L-PN-83)[1]. Results of test linearity of 10-stages and 8-stages R5900 PMTs. by: Crouau, M; Garnier, E; Montarou, G; - 13 Sep 1996


[1] *http://atlasinfo.cern.ch/Atlas/SUB_DETECTORS/TILE/tileref/tileref.html*

[9] ATL-TILECAL-99-012. (ATL-COM-TILECAL-99-012)[1]. Simulation of the photomultiplier response, by: I. Fedorko, S.Tokar and I. Chirikov-Zorin - 19 May 1999, CERN
[10] ATL-TILECAL-97-108. (ATL-L-PN-108)[1]. Characterization of the Hamamatsu 10-stages R5900 photomultipliers at Clermont for the TILE calorimeter. by: Bouhemaid,N; Crouau,M; Gil Botella,A; Gonzalez de la Hoz; Grenier,P; Montarou,G; Muanza,G.S; Poirot,S; Vazeille,F; - 28 Apr 1997
[11] G. Barbiellini, A.Martins, F.Scuri, A simulation study of the behavior of fine photomultipliers in magnetic field, Nucl Instrum Meth., A362(1996) p. 245
[12] Application Software Group, CERN Program Library, 1995, CERN, Geneva, Switzerland.
[13] I.S. Gradshteyn and I.M. Ryzhik, Table of Integrals, Series, and Products, 5th ed., Academic Press, 1994.

Received by Publishing Department
on September 8, 2000.

[1] *http://atlasinfo.cern.ch/Atlas/SUB_DETECTORS/TILE/tileref/tileref.html*

Чириков-Зорин И.Е. и др. E13-2000-213

Прецизионный метод анализа одноэлектронных спектров фотоумножителя в металлическом корпусе

Предложена усложненная функция отклика фотоумножителя для анализа одноэлектронных спектров компактного фотоумножителя в металлическом корпусе. Представленным методом анализировались спектры фотоумножителя R5600 (Hamamatsu). Детальный анализ показал, что метод достоверно описывает процесс умножения заряда в этих фотоумножителях и может быть использован для определения их основных внутренних параметров.

Работа выполнена в Лаборатории ядерных проблем им. В.П.Джелепова ОИЯИ.

Препринт Объединенного института ядерных исследований. Дубна, 2000

Chirikov-Zorin I.E. et al. E13-2000-213

Method for Precise Analysis of the Metal Package Photomultiplier Single Photoelectron Spectra

A sophisticated photomultiplier responce function was suggested for single photoelectron analysis of the compact metal package photomultiplier spectra. The spectra taken by Hamamatsu R5600 photomultipliers have been analysed by the presented method. The detailed analysis shows that the method appropriately describes the process of charge multiplication in these photomultipliers and can be used to find their basic internal parameters.

The investigation has been performed at the Dzhelepov Laboratory of Nuclear Problems, JINR.

Preprint of the Joint Institute for Nuclear Research. Dubna, 2000

Макет Т.Е.Попеко

Подписано в печать 02.10.2000
Формат 60 × 90/16. Офсетная печать. Уч.-изд. листов 2,56
Тираж 320. Заказ 52260. Цена 3 р.

Издательский отдел Объединенного института ядерных исследований
Дубна Московской области